

QUT Digital Repository:  
<http://eprints.qut.edu.au/>



This is the accepted version of this conference paper. Published as:

Tesfamichael, Tuquabo (2009) *Electron beam evaporation of tungsten oxide films for gas sensors*. In: Proceedings of the IEEE Sensors 2009 Conference, 25-28 October 2009, Christchurch Convention Centre, Christchurch.

© Copyright 2009 IEEE

# Electron Beam Evaporation of Tungsten Oxide Films for Gas Sensors

T. Tesfamichael

Queensland University of Technology

Faculty of Built Environment and Engineering, School of Engineering Systems

Brisbane, Australia

email: [t.tesfamichael@qut.edu.au](mailto:t.tesfamichael@qut.edu.au)

**Abstract**—Pure and Iron incorporated nanostructured Tungsten Oxide ( $\text{WO}_3$ ) thin films were investigated for gas sensing applications using noise spectroscopy. The  $\text{WO}_3$  sensor was able to detect lower concentrations (1 ppm-10 ppm) of  $\text{NH}_3$ , CO,  $\text{CH}_4$  and Acetaldehyde gases at higher operating temperatures between  $100^\circ\text{C}$  to  $250^\circ\text{C}$ . The response of the  $\text{WO}_3$  sensor to  $\text{NH}_3$ ,  $\text{CH}_4$  and Acetaldehyde at lower temperatures ( $50^\circ\text{C}$ - $100^\circ\text{C}$ ) was significant when the sensor was photo-activated using blue-light emitting diode (Blue-LED). The  $\text{WO}_3$  with Fe ( $\text{WO}_3:\text{Fe}$ ) was found to show some response to Acetaldehyde gas only at relatively higher operating temperature ( $250^\circ\text{C}$ ) and gas concentration of 10 ppm.

## I. INTRODUCTION

Gas sensors are of great importance for many applications including industrial production, environmental monitoring, medical diagnosis, domestic security, etc. There are several gasses known to be harmful to humans and the environment and to protect people and the environment from these harmful gases affordable gas sensors with higher detecting capacity and gas selectivity are needed. Such devices are suitable to detect the presence of low concentration target gasses and give warnings or send message for proper action when the designed threshold value is attained. For example health related problems may result from low indoor air quality due to various pollutants and immediate ventilation of these species is desirable when the limit is reached [1]. Thin film sensors are widely compatible to microelectronic technology and can easily be integrated into different types of circuits. Most of research in gas sensing devices has been focused on metal oxide materials such as  $\text{SnO}_2$ ,  $\text{TiO}_2$ ,  $\text{ZnO}$  and  $\text{WO}_3$  because of their simplicity and low cost. The gas sensing properties of these types of oxides are determined by their intrinsic properties, addition of impurities into the oxides and film microstructure including particle size, distribution and orientation, surface morphology and porosity.

Thin films are usually compact and the active layer is limited to the surface whereas thick films are commonly porous and hence the whole layer can interact with the gas species. If a controlled porosity can be achieved, then the gas sensing properties of thin films can be enhanced by depositing films of nanostructured grain size. From a theoretical study elsewhere, the sensitivity for gas detection can be significantly enhanced if the grain size is smaller than 50 nm [2]. Film thickness can have significant effect in optimizing sensor selectivity and sensitivity [3]. Gas detecting sensitivity also depends on the reactivity of film surface as sensors are strongly influenced by the presence of oxidizing or reducing gases on the surface. The reactivity can be enhanced by impurities, defects and active species

on the surface of the films, increasing the adsorption of gas species. It has been shown that inclusion of different doping metals in the oxide films increased the sensitivity to specific gases [4-7]. Recent research reports show that room temperature gas detection of metal oxide sensors can be enhanced based on photo-activation of the metal oxide film. In most of the work a UV-light had been used to activate and increase gas selectivity and sensitivity [8]. Gas detection capacity can also be enhanced by mixing metal oxides since each material has its own response and the mixture can add sensitivity and selectivity to specific gas species and also often improves sensor quality and performance. An increase of response towards certain gasses has been reported elsewhere, when iron oxide was added into tungsten oxide film [9].

The main objective of this experiment is to investigate the gas detection capacity and sensitivity of an electron beam evaporated nanostructured  $\text{WO}_3$  thin film and its effect when 10at% of iron is incorporated into the tungsten oxide film ( $\text{WO}_3:\text{Fe}$ ). The film development and preparations have been reported elsewhere [10]. In addition, this paper investigates low temperature gas detection of the  $\text{WO}_3$  and  $\text{WO}_3:\text{Fe}$  sensors when photo-activated using blue-light emitting diode (Blue-LED). The gas sensitivity and selectivity of the  $\text{WO}_3$  and  $\text{WO}_3:\text{Fe}$  sensors were performed using noise spectroscopy.

## II. FILM PROPERTIES

Fig. 1 shows AFM images of  $\text{WO}_3$  and  $\text{WO}_3:\text{Fe}$  films annealed at  $300^\circ\text{C}$  for 1 hour. The average particle diameter (film roughness) of these samples as estimated using the Nova and Image Analysis software were 9 nm (2.61 nm) and 12 nm (2.93 nm), respectively. In order to enhance the gas-sensing characteristic of a film optimum grain size and porosity are needed.

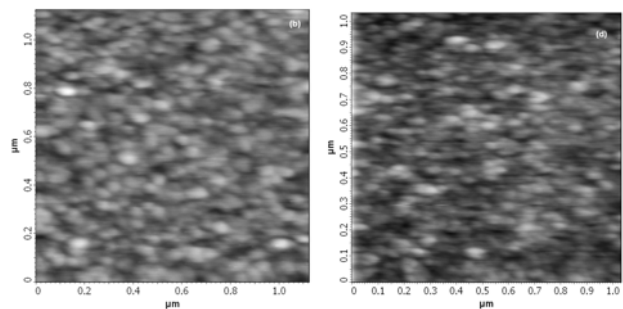


Figure 1. AFM images of  $\text{WO}_3$  (left) and  $\text{WO}_3:\text{Fe}$  (right) films heat treated at  $300^\circ\text{C}$  for 1 hour.

The chemical nature of the films were determined using X-Ray Photo-electron Spectroscopy (XPS) and Raman spectroscopy. The

XPS core level of W  $4f_{7/2}$  peaks for the  $WO_3$  and  $WO_3:Fe$  samples were measured at binding energies of 36.2 eV and 35.9 eV, respectively. The Fe 2p spectrum of the annealed  $WO_3:Fe$  contained peak of iron oxides which resulted from  $Fe^{+3}$  species. Raman peaks of the annealed sample were found at peak positions about  $957\text{ cm}^{-1}$  and  $779\text{ cm}^{-1}$ , respectively (Fig. 2). From the Raman characteristics band, the short range order of the annealed films may be assigned to the tetragonal-phase. The addition of Fe to  $WO_3$  seems to prompt the formation of crystalline grains, as seen from the Raman intensity and the AFM images reported elsewhere [10].

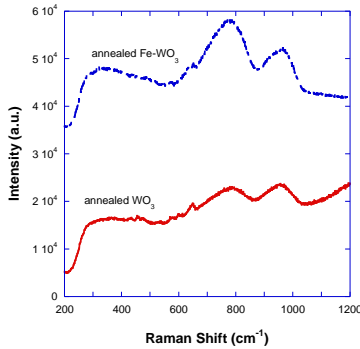


Figure 2. Raman spectra of annealed  $WO_3$  and  $WO_3:Fe$  films measured using 532 nm NdYAG laser source and a power of 5 mW at the sample.

### III. GAS SENSING CHARACTERISTICS

The gas sensing properties of two types of sensors ( $WO_3$  and  $WO_3:Fe$  sensors) as a function of operating temperature, types of gas and concentrations have been studied using noise spectroscopy. The gas sensing measurements were performed inside a  $1\text{ dm}^3$  volume stainless steel chamber connected to a low-noise current generator. The resistance and voltage fluctuation across the sensor were measured using digital multimeter and Stanford SR560 low-noise differential preamplifier, respectively. The later (voltage fluctuation) was sampled with a rate of 50 kHz by a PowerLab/4SP (AD Instruments) data acquisition unit and calculated a Power Density Spectrum (PDS). A gas calibration system with mass flow controllers was used to allow continuous flow of known concentration gas into the chamber after a steady background reference signal in synthetic air was established. The total flow rate was kept constant at about 405 sccm. The PDS of a particular gas was then measured when the Stochastic signal remained constant as a function of time. The PDS signal obtained from the noise spectroscopy measurements was used to determine the gas sensitive and selectivity of the sensors using synthetic air as reference. The performance of both sensors to different target gasses ( $NH_3$ ,  $CO$ ,  $CH_4$  and Acetaldehyde) were tested in the concentration range of 1 - 10 ppm and operating temperature  $100^\circ\text{C}$ - $250^\circ\text{C}$ . In addition, the performances of the sensors at lower temperatures ( $50^\circ\text{C}$ - $100^\circ\text{C}$ ) were investigated by assisting the sensors with blue-light emitting diode (Blue-LED).

In most of the measurements, the time needed to reach a steady state signal of the target gas was in the range of about 10-15 minutes and the time taken to achieve the background signal after cutting-off the target gas was about 5-10 minutes. Fig. 3 is an example of  $WO_3$  sensor exposed to 10 ppm  $NH_3$  gas at  $200^\circ\text{C}$  for different times between 3 to 15 minutes in which saturation of the signal occurred after 10 minutes. It has been reported elsewhere that the change in stochastic signal when the film is exposed to a target gas, is due to resistance fluctuation of the film and not by other effects [11]. A

common problem with a nanoparticle-based sensors is their long-term drift of the electrical resistance in which the noise spectroscopy method using PDS can be an alternative technique for gas detection measurements. The PDS spectra obtained at higher temperatures tend to bend in the lower frequency range and the reason for this was not known and needs further understanding of the spectroscopy signal.

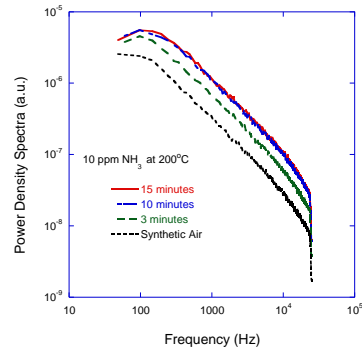


Fig. 3 Power Density Spectra (PDS) of  $WO_3$  sensor exposed to 10 ppm  $NH_3$  at  $200^\circ\text{C}$  for different times between 3-15 minutes.

#### A. $NH_3$ Gas Detection of $WO_3$ Sensor

In the present time, study of ammonia ( $NH_3$ ) gas sensor has greatly increased as it is one of the industrial gasses with high toxicity. Temperature dependence spectra of the  $WO_3$  sensor exposed to 10 ppm of  $NH_3$  operated at  $250^\circ\text{C}$ ,  $150^\circ\text{C}$  and  $100^\circ\text{C}$  are shown in Fig. 4. The gas detection capacity of the sensor was observed over a wide temperature range at higher temperatures. The detection of the sensor at lower temperature ( $100^\circ\text{C}$ ) was significant when the sensor was photo-activated using Blue-LED (Fig. 4c). To the best of my knowledge this is the first to observe the enhancement of low concentration gas at low temperatures using Blue-LED method. The optical band-gap energy ( $E_g$ ) of the  $WO_3$  film as measured previously [10] was in the UV/Vis part of the solar spectrum (3.12 eV or  $0.38\text{ }\mu\text{m}$ ) and such lower  $E_g$  can be suitable for photo activated sensors.

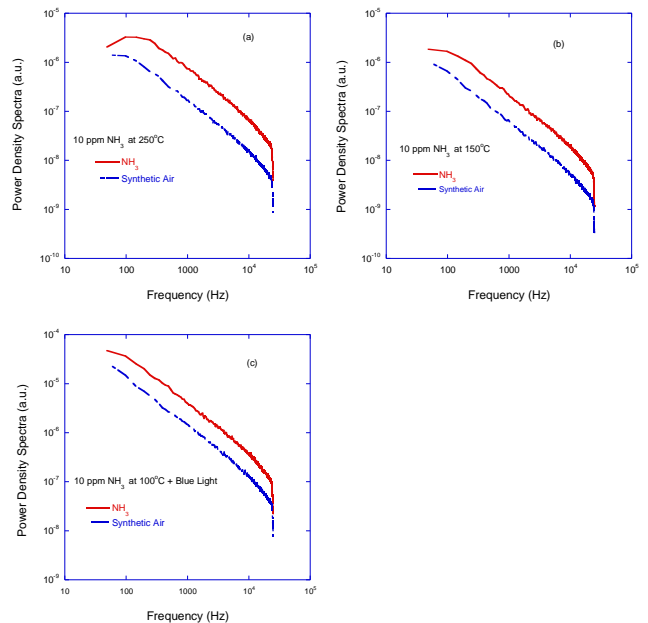


Figure 4. Power Density Spectra (PDS) of  $WO_3$  sensor exposed to 10 ppm  $NH_3$  at (a)  $250^\circ\text{C}$ , (b)  $150^\circ\text{C}$ , (c)  $100^\circ\text{C}$  + Blue-LED.

## B. CO Gas Detection of $WO_3$ Sensor

The toxic nature of CO necessitates the detection of this gas for household and environmental applications and for controlling emissions from combustion processes [3]. Fig. 5 shows the response of  $WO_3$  sensor to 1 ppm of CO gas measured at higher operating temperatures between 100°C to 250°C. As shown in the figures, the  $WO_3$  sensor exhibits low sensitivity for all the measured temperature range. This indicates that the  $WO_3$  sensor is less sensitive to CO at lower concentrations. However, at higher concentration (10 ppm) and higher operating temperature ( $>200^\circ\text{C}$ ) some appreciable response towards CO was observed as shown in Fig. 6. The stochastic signal increases with increasing gas concentration and the change in the signal is directly related to the concentration of the exposed gas. At lower operating temperature (50°C), small amount of signal was detected for higher CO concentration (10 ppm) only after illumination the sensor using Blue-LED (Fig. 6d).

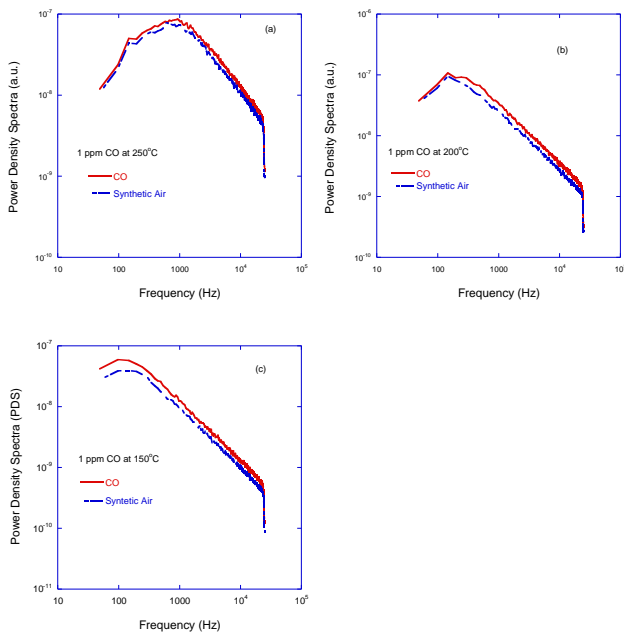


Figure 5. Power Density Spectra (PDS) of  $WO_3$  sensor exposed to 1 ppm CO at (a) 250°C, (b) 200°C, and (c) 150°C.

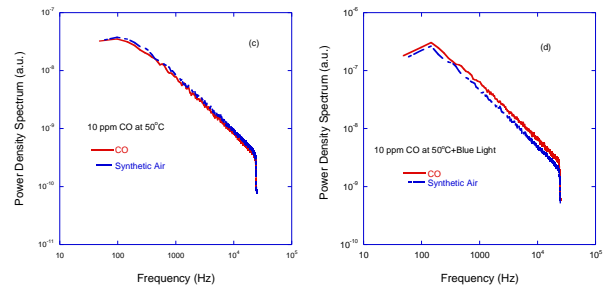
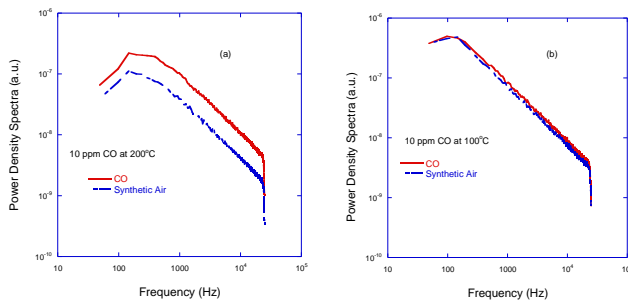


Figure 6. Power Density Spectra (PDS) of  $WO_3$  sensor exposed to 10 ppm CO at (a) 200°C, (b) 100°C, (c) 50°C, and (d) 50°C+ Blue-LED.

## C. $CH_4$ Gas Detection of $WO_3$ sensor

Methane is one of the green house gases and hence requires environmental monitoring using gas sensors. The detection of the  $WO_3$  sensor towards 1 ppm and 10 ppm  $CH_4$  gas at room temperature with and without blue light illumination are shown in Fig. 7a-b. A significant response was observed when the sensor was photo-activated with Blue-LED. The response increases with increasing the concentration of the gas from 1 ppm to 10 ppm. For comparison photo-activation of the sensor with UV-LED was performed and the detected signal for a 10 ppm  $CH_4$  gas is shown in Fig. 7c. From the results, it can observe that the Blue-LED is more efficient than the UV-LED although both LEDs have similar intensity.

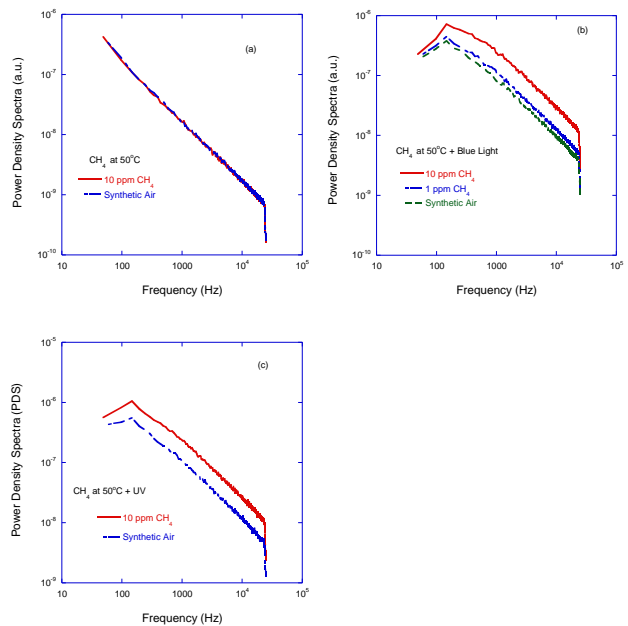


Figure 7. Power Density Spectra (PDS) of  $WO_3$  sensor exposed to  $CH_4$  at 50°C (a) without external light, (b) with Blue-LED and (c) with UV-LED.

## D. Acetaldehyde Gas Detection of $WO_3$ Sensor

Acetaldehyde has received much attention as a hazardous and odorous substance in studies of air pollution as it is one of the 33 air pollutants indicated by the U.S. Environmental Protection Agency and considered being a probable carcinogen. The temperature dependence spectra of the  $WO_3$  sensor exposed to 10 ppm Acetaldehyde operated at various temperatures (150°C and 200°C)

are shown in Fig. 8. The gas detection capacity of the sensor was large over a wide temperature range with optimum temperature around 200°C.

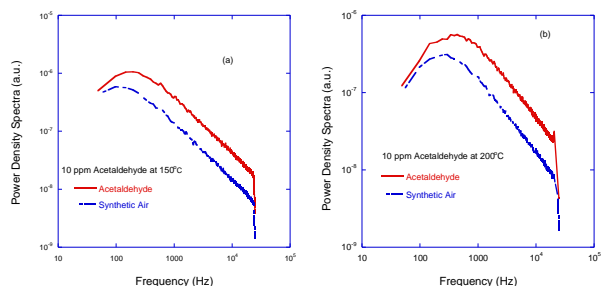


Figure 8. Power Density Spectra (PDS) of  $WO_3$  sensor exposed to 10 ppm Acetaldehyde at (a) 150°C and (b) 200°C.

### E. Gas Detection of $WO_3:Fe$ Sensor

Mixed-metal-oxide sensor was obtained by annealing the  $WO_3:Fe$  sample at 300°C in air for 1 hour and its response to various gasses ( $NH_3$ ,  $CO$ ,  $CH_4$  or Acetaldehyde) has been tested. There was no response of the sensor towards  $NH_3$ ,  $CO$  and  $CH_4$  gases measured in the concentration range of 1 ppm to 10 ppm and at operating temperature between 100°C to 250°C. Fig. 9a shows PDS of the  $WO_3:Fe$  sensor exposed to 1 ppm  $CO$  at operating temperature of 200°C. The highest response observed was for 10 ppm Acetaldehyde gas at operating temperature of 250°C (Fig. 9b). This may indicate to a certain degree the gas selectivity of the sensor. Thus, the response of tungsten oxide sensor toward  $NH_3$ ,  $CO$ ,  $CH_4$  and Acetaldehyde gases has been diminished when 10at% of iron was added.

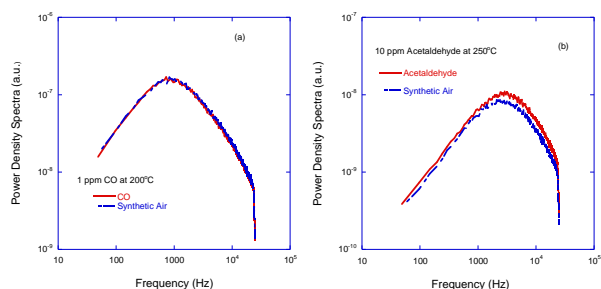


Figure 9. Power Density Spectra (PDS) of  $WO_3:Fe$  sensor exposed to (a) 1 ppm  $CO$  at 200°C, and (b) 10 ppm Acetaldehyde gas at 250°C.

## IV. CONCLUSIONS

Thin film nanostructured  $WO_3$  and  $WO_3:Fe$  gas sensors have been developed using electron beam evaporation process. The gas sensing characteristics of the films after annealing at 300°C for 1 hour have been studied to  $NH_3$ ,  $CO$ ,  $CH_4$  and Acetaldehyde. Experimental results indicate that the pure  $WO_3$  sensor has good sensitivity to these gases in the range of 1-10 ppm and higher operating temperatures (150°C-250°C). In addition, the sensitivity of the  $WO_3$  sensor at lower temperatures (50°C-100°C) has been observed when the sensor was photo-activated with Blue-LED. From the results, it can be concluded that photo-activated  $WO_3$  thin film indicated a promising gas sensor device that can operate at room temperature. The mixed metal oxide sensor of  $WO_3:Fe$  showed sensitivity to Acetaldehyde gas only and further investigation may be needed to determine its sensitivity and selectivity to other gases. The overall results indicate that the  $WO_3$  sensor exhibit

reproducibility for the detection of various gasses during the many cycles of tests. An interesting finding in this project is that, gas sensors are commonly operated at higher temperatures (>200°C) but the nanostructured thin film  $WO_3$  gas sensor devices developed in this paper were found to be sensitive to target gasses at lower temperatures (50°C to 100°C) when illuminated with Blue-LED.

## ACKNOWLEDGMENT

The author is indebt, to the Japanese Society for the Promotion of Science (JSPS) for the financial assistance to do research in this project at Hokkaido University (Sapporo), and to the Solid State Physics (FTF-group) in Uppsala University (Uppsala) for allowing further research at the Angstrom Laboratory. This research was done during my Professional Development Leave offered by Queensland University of Technology (Brisbane).

## REFERENCES

- [1] C. G. Granqvist, A. Azens, P. Heszler, L. B. Kish, L. Osterlund, "Nanomaterials for benign indoor environments: Electrochromics for "smart windows", sensors for air quality, and photocatalysts for air cleaning," *Solar Energy Materials and Solar Cells* **91**, 355 (2007).
- [2] X. Wang, S. S. Yee, W. P. Carey, "Transition between neck-controlled and grain-boundary-controlled sensitivity of metal-oxide gas sensors," *Sensors and Actuators B: Chemical* **25**, 454 (1995).
- [3] G. G. Mandayot *et al.*, "Strategies to enhance the carbon monoxide sensitivity of tin oxide thin films," *Sensors and Actuators B: Chemical* **95**, 90 (2003).
- [4] H. Kawasaki, T. Ueda, Y. Suda, T. Ohshima, "Properties of metal doped tungsten oxide thin films for  $NO_x$  gas sensors grown by PLD method combined with sputtering process," *Sensors and Actuators B: Chemical* **100**, 266 (2004).
- [5] V. Khatko *et al.*, "Gas sensing properties of nanoparticle indium-doped  $WO_3$  thick films," *Sensors and Actuators B: Chemical* **111-112**, 45 (2005).
- [6] L. J. LeGore *et al.*, "Defects and morphology of tungsten trioxide thin films," *Thin Solid Films* **406**, 79 (2002).
- [7] M. A. Ponce, C. M. Aldao, M. S. Castro, "Influence of particle size on the conductance of  $SnO_2$  thick films," *Journal of the European Ceramic Society* **23**, 2105 (2003).
- [8] B. P. J. de Lacy Costello, R. J. Ewen, N. M. Ratcliffe, M. Richards, "Highly sensitive room temperature sensors based on the UV-LED activation of zinc oxide nanoparticles," *Sensors and Actuators B: Chemical* **134**, 945 (2008).
- [9] E. Comini, L. Pandolfi, S. Kaciulis, G. Faglia, G. Sberveglieri, "Correlation between atomic composition and gas sensing properties in tungsten-iron oxide thin films," *Sensors and Actuators B: Chemical* **127**, 22 (2007).
- [10] T. Tesfamichael, M. Arita, T. Bostrom, J. M. Bell, "Characterization of Electron-Beam Evaporated Tungsten Oxide Films for Gas Sensor Applications," unpublished, (2008).
- [11] J. S. Bendat, A. G. Piersil, *Random Data Analysis and Measurement Procedures*. (Wiley, New York, USA, 2000).